NEW WAVEGUIDE STRUCTURES FOR MILLIMETER-WAVE INTEGRATED CIRCUITS

Tatsuo Itoh and Raj Mittra
Department of Electrical Engineering and
Coordinated Science Laboratory
University of Illinois
Urbana, Illinois 61801

Abstract

Three new types of waveguide structures, which are useful for millimeter-wave integrated circuits, have been studied. Methods of analysis for these structures have been developed and the numerical results have been compared with experimental data.

Introduction

Recently, much interest has been demonstrated in the study of millimeter-wave integrated circuits (MWIC) [1,2,3]. The waveguide structures for MWIC may be classified into two broad categories: microstrip type [1] and dielectric waveguide type [2,3]. One of the advantages of the latter is its ease of fabrication since the cross-sectional dimension is of the order of the wavelength, much larger than for microstrip structures. On the other hand, microstrip structures are more convenient for mounting solid-state devices because of the presence of conductors.

In this paper we analyze three new types of waveguides which are potentially useful for millimeter-wave IC's (Fig. 1). They are basically dielectric waveguides in the sense that the major portion of the electromagnetic energy flow is in the dielectric material away from the conductor, and yet the presence of the conductor provides a convenient means of d.c. biasing circuits and heat sinks for solid-state devices.

Description and Analysis of Waveguides

Double-layer slot line

The original version of the slot line, which was proposed by Cohn [4], has a slot in the conductor which is, in turn, backed by a dielectric substrate. In the present structure, an additional layer of dielectric material is provided. Since the relative dielectric constant ε_{r2} of Region 2 is chosen to be larger than that of Region 1, most of the power flow is in Region 2. Moreover, in the x-direction, the field is concentrated in the vicinity of the slot.

The analysis of the dispersion characteristic has been carried out by an extension of the method used for conventional slot lines by Itoh and Mittra [5]. The total field in the structure is first expressed in terms of TE and TM components. Next, we introduce the Fourier transform via the equation

$$\tilde{\phi}(\alpha,y) = \int_{-\infty}^{\infty} \phi(x,y)\, \alpha^{-j\alpha x}\, dx \quad .$$

Instead of solving the boundary value problem associated with the structure in the space domain, the analytical process is carried out in the Fourier transform domain. When all the boundary conditions are applied to the field expression in the transform domain, one obtains the following equations

$$\tilde{K}_{xx}\,\tilde{E}_x + \tilde{K}_{xz}\,\tilde{E}_z = \tilde{J}_x \qquad (1a)$$

$$\tilde{K}_{zx}\,\tilde{E}_x + \tilde{K}_{zz}\,\tilde{E}_z = \tilde{J}_z \qquad (1b)$$

where $\tilde{E}_x$ and $\tilde{E}_z$ are Fourier transforms of the tangential aperture E field components, $\tilde{J}_x$ and $\tilde{J}_z$ are transforms of surface current components on the ground plane, and $\tilde{K}_{xx}$ etc. are known functions of transform variable α and unknown propagation constant k_z. Equations (1a) and (1b) are solved by the application of Galerkin's method in the transform domain. From this method, a set of homogeneous simultaneous equations is obtained. The eigenvalue equation for k_z is then derived by equating to zero the determinant of the coefficient matrix of the simultaneous equations. The values of k_z for a given frequency are obtained by numerically solving the eigenvalue equation.

Insulated image guide

In this structure, an additional layer of dielectric material is inserted between the dielectric rod and the ground plane of the conventional image guide. This idea has been used in the "insular" line developed at IIT Research Institute [3]. However, in the present structure, the choice of dielectric constants and physical dimensions are somewhat more arbitrary, though inequality $\varepsilon_{r1} > \varepsilon_{r2}$ is required to concentrate the energy flow in the dielectric rod away from the ground plane. Since the analysis method of this waveguide is quite similar to the strip dielectric guide explained below, it will not be presented here and only the major deviations from the strip dielectric guide analysis will be indicated in the next section.

Strip dielectric waveguide

The concept of this waveguide is entirely new. Although the structure looks similar to the insulated image guide mentioned earlier, the wave propagation mechanism is somewhat different. Since $\varepsilon_{r2} > \varepsilon_{r1}$ and $\varepsilon_{r2} > \varepsilon_{r3}$, most of the energy flow is in the layer with dielectric constant ε_{r2}. The strip (ε_{r1}) provides the lens effect in the transverse direction; hence, most of the energy flow is immediately below the strip. The presence of the ground plane is convenient for mounting solid-state devices, and yet the conductor loss is minimized due to the presence of substrate layer (ε_{r3}). Since most of the energy propagates in the dielectric layer which is easily fabricated, the radiation loss due to mechanical irregularities on the side walls of the dielectric strip is expected to be much smaller when compared to

the image guide type lines. A similar idea has been used in the transmission line for optical integrated circuits [6].

To analyze the waveguide, a concept of effective dielectric constants, which has previously been used by Toulios and Knox [2], is extended here to apply to the new structure. There are two sets of modes, E^y and E^x types. Since both modes are similar, we will only discuss the E^y mode problem. If Regions I, II and III are infinitely long in the x-direction, we have three multilayered slab waveguides. The propagation constants $k_{z1} = k_{z3}$ and k_{z2} in these slab waveguides for a given frequency may be easily derived from the eigenvalue equations for surface-wave modes. For instance, in the slab waveguide corresponding to Region I, the E_y field is proportional to

$$\phi = A\, e^{-\eta(y-d-t)}\, e^{-jk_{z1}z} \qquad y > d + h$$

$$(B \cos k_y y + C \sin k_y y)\, e^{-jk_{z1}z} \qquad h < y < d + h$$

$$D \cosh \xi y\, e^{-jk_{z1}z} \qquad 0 < y < h$$

$$k_{z1}^2 = \varepsilon_{r2} k_0^2 - k_y^2 = \varepsilon_{r3} k_0^2 + \xi^2 = k_0^2 + \eta^2, \quad k_0 = 2\pi/\lambda .$$

If one matches the tangential field at the interfaces y = d, and d + h, the eigenvalue equation is easily derived. Let us define the effective dielectric constant in Region I as

$$\varepsilon_{e1} = \left(\frac{k_{z1}}{k_0}\right)^2 = \varepsilon_{r2} - \left(\frac{k_y}{k_0}\right)^2 .$$

ε_{e2} for Region II may be similarly derived. The effective dielectric constant may be interpreted as that of a hypothetical medium in which a plane wave propagates at the same phase velocity as the surface wave in the original structure. After ε_{e1} $(= \varepsilon_{e3})$ and ε_{e2} are derived, we replace the original waveguide structure by the hypothetical structure shown in Fig. 2(b). The propagation constant k_z of the original structure is obtained by solving the eigenvalue equation of the surface-wave mode in the hypothetical structure (b).

Finally, let us briefly describe the application of the effective dielectric constant approach to the insulated image guide problem [Fig. 1(b)]. In the insulated image guide, most of the energy is in the rod and the energy in the substrate is negligible except for the region immediately below the rod. Hence, $\varepsilon_{e1} = \varepsilon_{e3}$ may be set equal to unity. It is only necessary to obtain ε_{e2} by solving an eigenvalue equation for a slab waveguide corresponding to the region containing the rod.

Numerical Results and Experimental Data

Numerical results for the propagation constant of three types of waveguides have been obtained and some typical results are presented in Figs. 3, 4 and 5. Experiments have been performed at the X band in order to check the accuracy of the present methods of solution and the numerical results. For the slot line, the propagation constant was found by a short-circuited slot line whose length was variable. In the case of two other waveguides, the standing wave patterns have been measured by detecting the leakage field of the open-ended dielectric waveguides. Note that in the strip dielectric guide, h was set to zero for simplicity of computation and experimental work. Numerical results agree well with the experimental data for all three cases. In addition, numerical and experimental results for field distributions are also included in the paper.

Conclusions

Descriptions and analysis methods have been presented for three new types of waveguides potentially useful for millimeter-wave integrated circuits. It should be noted that the effective dielectric constant approach, although simple, is only an approximate technique and works well when the aspect ratio of strip or rod (W/t) is large and the difference between ε_{r1} and ε_{r2} is small. Further, it is not a good approximation for higher-order modes. In the future, more exact analysis as well as loss calculations are being planned.

References

1. M. V. Schneider, "Millimeter-wave integrated circuits," 1973 IEEE G-MTT Symposium Digest, pp. 16-18.

2. P. P. Toulios and R. M. Knox, "Rectangular dielectric image lines for millimeter integrated circuits," Western Electric Show and Convention, Los Angeles, California, August 25-28, 1970.

3. M. M. Chrepta and H. Jacobs, "Millimeter-wave integrated circuits," Microwave Journal, vol. 17, pp. 45-47, November 1974.

4. S. B. Cohn, "Slot line on a dielectric substrate," IEEE Trans. Microwave Theory Tech., vol. MTT-17, pp. 768-778.

5. T. Itoh and R. Mittra, "Dispersion characteristics of the slot lines," Electronics Letters, vol. 7, pp. 364-365, July 1971.

6. H. Noda, H. Furuta, and A. Ihaya, "A novel optical waveguide for integrated optics," IEEE/OSA Conference on Laser Engineering and Applications, Washington, D.C., May 30-June 1, 1973.

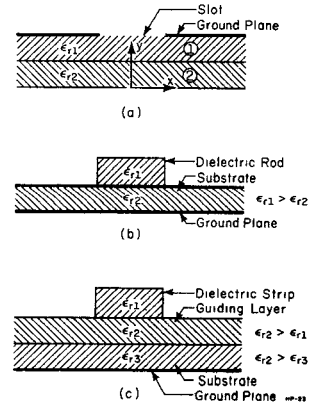

Fig. 1. (a) Double-layer slot line, (b) Insulated image guide, (c) Strip dielectric waveguide.

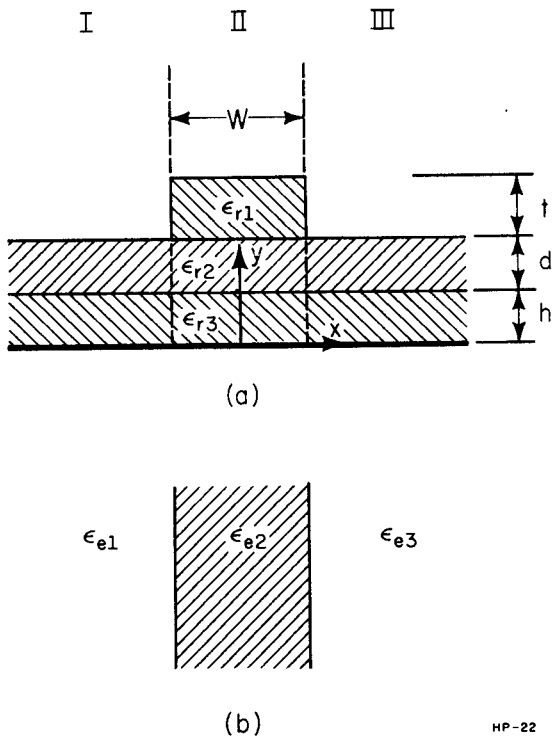

Fig. 2. (a) Cross section of strip dielectric guide, (b) Equivalent slab waveguide.

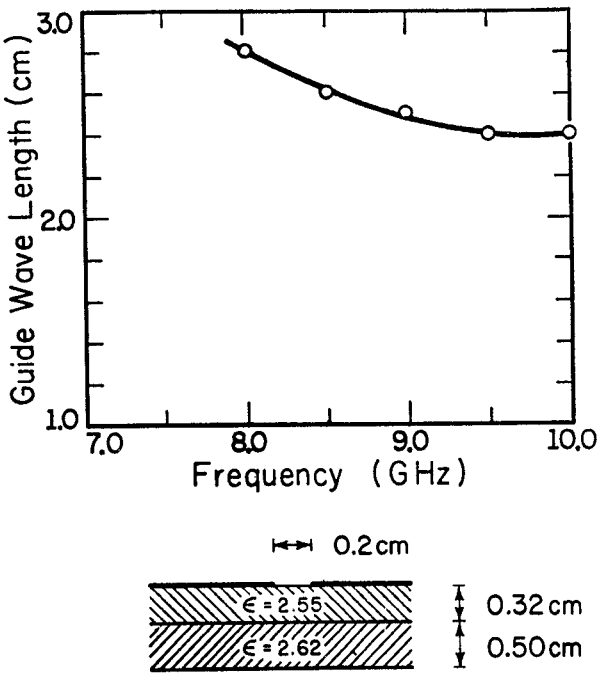

Fig. 3. Dispersion characteristics of double-layer slot line.

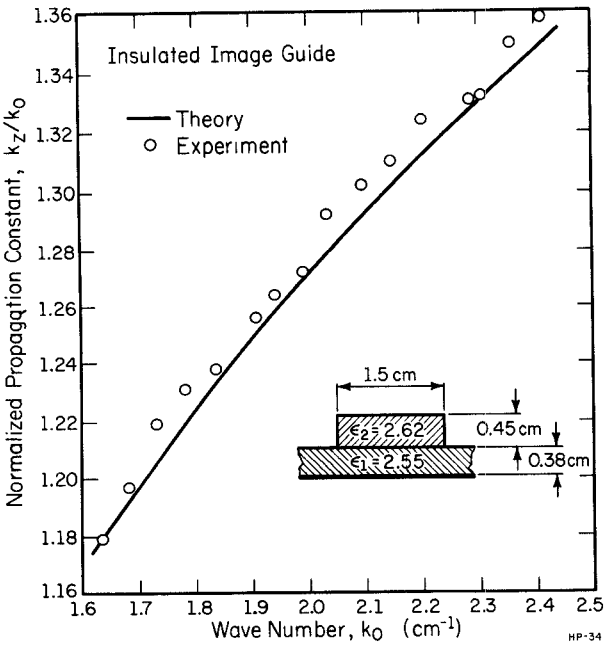

Fig. 4. Dispersion characteristics of insulated image guide.

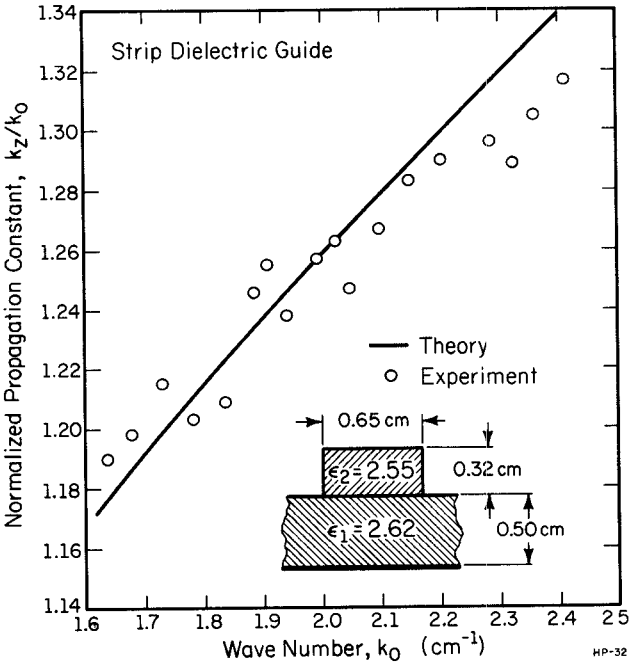

Fig. 5. Dispersion characteristics of strip dielectric guide.

Acknowledgment

This work was supported in part by Joint Services Electronics Program DAAB C-0259 and in part by U. S. Army Research Grant DAHC04-74-G0113.